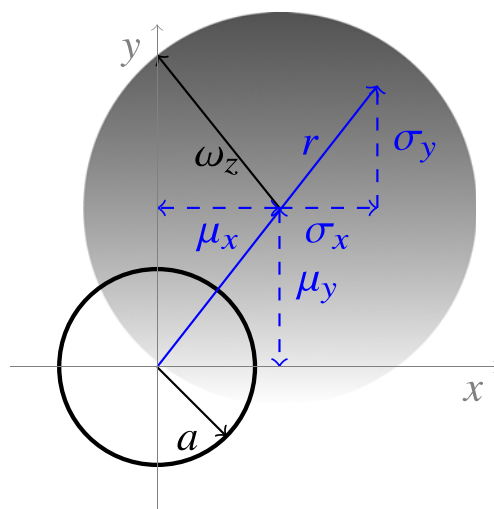


On the Effect of Correlated Sways on Generalized Misalignment Fading for Terrestrial FSO Links

Volume 9, Number 3, June 2017

Rubén Boluda-Ruiz
Antonio García-Zambrana
Beatriz Castillo-Vázquez
Carmen Castillo-Vázquez



DOI: 10.1109/JPHOT.2017.2694707
1943-0655 © 2017 IEEE

On the Effect of Correlated Sways on Generalized Misalignment Fading for Terrestrial FSO Links

Rubén Boluda-Ruiz,¹ Antonio García-Zambrana,¹
Beatriz Castillo-Vázquez,¹ and Carmen Castillo-Vázquez²

¹Andalucía Tech, Department of Communications Engineering, Campus de Teatinos,
University of Málaga, Málaga 29701, Spain

²Andalucía Tech, Department of Mathematical Analysis, Statistics and Operations Research
and Applied Mathematics, Campus de Teatinos, University of Málaga, Málaga 29701, Spain

DOI:10.1109/JPHOT.2017.2694707

1943-0655 © 2017 IEEE. Translations and content mining are permitted for academic research only.
Personal use is also permitted, but republication/redistribution requires IEEE permission. See
http://www.ieee.org/publications_standards/publications/rights/index.html for more information.

Manuscript received March 1, 2017; accepted April 11, 2017. Date of publication April 17, 2017; date of current version April 27, 2017. This work was supported by the Universidad de Málaga. Corresponding author: R. Boluda-Ruiz (e-mail: rbr@ic.uma.es).

Abstract: Terrestrial free-space optical (FSO) links are severely damaged by both atmospheric turbulence and misalignment errors. Generally, the optic community models misalignment by considering two different axes, i.e., the horizontal displacement and the elevation, as independent Gaussian random variables (RVs), whose probability density function is the well-known Beckmann distribution in the general case. In the current paper, we generalize this previous approach by misalignments with correlated sways since both the horizontal displacement and the elevation are not necessarily uncorrelated RVs in potential FSO applications. A statistical pointing error model is proposed, where not only is the laser beam width, detector size, and the effect of nonzero boresight and different jitter variances for each axes taken into account, but the effect of correlated sways is also taken into account. The proposed statistical model is used to evaluate the outage performance over gamma-gamma atmospheric turbulence channels. It is shown that the effect of correlation can only affect the coding gain when atmospheric turbulent is the dominant effect, while outage diversity is strongly dependent on correlation when pointing error is the dominant effect. Hence, correlation cannot be ignored in FSO systems. Simulation results are further included to confirm the analytical results.

Index Terms: Free-space optical (FSO), atmospheric turbulence, generalized pointing errors, correlated sways, gamma-gamma density function.

1. Introduction

Free-space optical (FSO) communication systems have attracted a considerable attention in recent years due to the ability to provide high speed links for a variety of applications as well as to establish terrestrial high-capacity wireless links that are demanded by the new wide-band telecommunication services. The main features are unlimited bandwidth, unlicensed-free spectrum, immunity to radio frequency (RF) interferences, robustness to eavesdropping and low cost. Furthermore, it can be expected that these systems will assume a noticeable role in the development of fifth-generation (5G) infrastructure, thus efficiently contributing to overcome the important challenge caused by the RF spectrum scarcity. This technology is able to transmit high-bandwidth data when fiber optic systems

are neither practical nor feasible. Commercially available systems offer capacities in the range of 100 Mbps to 2.5 Gbps. However, this technology is not without drawbacks: atmospheric turbulence and pointing errors the major challenging factors [1]. The effect of misalignment fading can result in a significant mismatch between transmitter and receiver of fixed-position laser communication systems. For instance, building sway due to wind loads, differential heating and cooling, or ground motion over time can lead to an important misalignment error [2], [3]. Additionally, pointing errors can also arise due to mechanical misalignment, errors in tracking systems, or due to mechanical vibrations present in the FSO system [4]. Different mitigation techniques such as narrower beam widths and automatic pointing and tracking systems have been used to avoid a high geometric loss when link distances greater than one kilometer are assumed [5], [6].

Over the last few years, the study of pointing errors in FSO communication systems has been quite an interesting subject for the optic community. Some statistical models have been presented, which have been used and continue using in a great deal of research articles [4], [7]–[12]. Recently, a new approximation of generalized pointing errors was proposed in [11], where pointing errors are modeled by the Beckmann distribution, presenting quite an useful tool to analyze the performance over atmospheric turbulence channels. The Beckmann distribution was also considered in [10] to evaluate the asymptotic ergodic capacity of FSO links over log-normal (LN) and gamma-gamma (GG) atmospheric turbulence channels, and in [12] to evaluate the outage performance over exponentiated Weibull (EW) atmospheric turbulence channels by using a moment generating function (MGF)-based approach. However, to the best of our knowledge, the effect of correlated sways on FSO link designs was never taken into account, i.e., both the horizontal displacement and the elevation have always been modeled as uncorrelated random variables (RVs). Generally, the radial displacement at the FSO receiver follows a Beckmann distribution as well as in other fields or applications. Hence, it seems much more reasonable to assume the effect of correlation between the horizontal displacement and the elevation since both of them are not necessarily uncorrelated in potential FSO applications. So far, the effect of correlated sways has only been assumed in satellite optical transmission when the radial displacement is distributed according to a Rayleigh distribution [13], [14].

In this work, for the first time, we characterize the outage performance over GG atmospheric turbulence channels under the presence of generalized pointing errors with correlated sways. In this way, we propose a new statistical model to describe the effect of correlated sways on pointing errors that is used to analyze the outage performance of FSO links. It must be noted that there are no published papers that address this challenging research problem. An approximate closed-form probability density function (PDF) for the composite GG atmospheric turbulence with generalized pointing errors is derived that serves as an analytical tool to evaluate the performance of any kind of FSO communications system with a higher degree of sophistication and realism. In light of the obtained results, we can conclude that the effect of correlated sways cannot be ignored in terrestrial FSO links since the correlation presents an important impact on the performance of FSO communication systems. Moreover, this study can be extended to other atmospheric statistical models such as LN and EW atmospheric turbulence channels, among others. Monte Carlo simulation results are further included in order to confirm the analytical results.

2. Effect of Correlated Sways

In this section, a statistical model to include the effect of correlated sways on misalignment fading will be established and analyzed in greater detail. The attenuation due to geometric spread and pointing errors can be approximated, as in [7], by

$$h_p(r; z) \approx A_0 \exp\left(-\frac{2r^2}{\omega_{z_{\text{eq}}}^2}\right), \quad r \geq 0 \quad (1)$$

where $v = \sqrt{\pi}a/\sqrt{2}\omega_z$, $A_0 = [\text{erf}(v)]^2$ is the fraction of the collected power at $r = 0$, a is the radius of a circular detection aperture, and $\omega_{z_{\text{eq}}}^2 = \omega_z^2 \sqrt{\pi} \text{erf}(v)/2v \exp(-v^2)$ is the equivalent beam width. The

beam width ω_z can be approximated by $\omega_z = \theta z$, where θ is the transmit divergence angle describing the increase in beam radius with distance from the transmitter.

We can express the radial displacement r at the receiver plane as $r^2 = x^2 + y^2$, where x and y represent the horizontal displacement and the elevation, respectively. The approximation in (1) is in good agreement with the exact value when the normalized beam width $\omega_z/a > 6$. Let us define a couple of useful pointing error parameters such as $\varphi_x = \omega_{z\text{eq}}/2\sigma_x$ and $\varphi_y = \omega_{z\text{eq}}/2\sigma_y$. These parameters are the ratios between the equivalent beam radius at the receiver and the corresponding pointing error displacement standard deviation (jitter) at the receiver.

Generally, the radial displacement r at the receiver is distributed according to the well-known Beckmann distribution when x and y are modeled as independent Gaussian RVs, whose integral-form PDF can be found in [15, (31)] as follows:

$$f_r(r) = \frac{r}{2\pi\sigma_x\sigma_y} \int_0^{2\pi} \exp\left(-\frac{(r\cos\theta - \mu_x)^2}{2\sigma_x^2} - \frac{(r\sin\theta - \mu_y)^2}{2\sigma_y^2}\right) d\theta, \quad r \geq 0. \quad (2)$$

As commented before, x and y are not necessarily uncorrelated RVs in terrestrial FSO applications. Both x and y can be modeled as correlated Gaussian RVs with different jitters for the horizontal displacement ($\sigma_x > 0$) and the elevation ($\sigma_y > 0$), and different boresight errors in each axis of the receiver plane ($\mu_x, \mu_y \in \mathbb{R}$), i.e., $x \sim N(\mu_x, \sigma_x)$ and $y \sim N(\mu_y, \sigma_y)$, and Pearson correlation coefficient $\rho \in [-1, 1]$. Then, the random vector (x, y) follows a bivariate normal distribution with mean vector (μ_x, μ_y) and covariance matrix

$$\begin{pmatrix} x \\ y \end{pmatrix} \sim N \left[\begin{pmatrix} \mu_x \\ \mu_y \end{pmatrix}, \begin{pmatrix} \sigma_x^2 & \rho\sigma_x\sigma_y \\ \rho\sigma_x\sigma_y & \sigma_y^2 \end{pmatrix} \right]. \quad (3)$$

It must be mentioned that for bivariate normal distribution, zero correlation implies independence. This is, of course, not so in general. The bivariate normal distribution for two related, normally distributed variables is defined by the following PDF:

$$f_{XY}(x, y) = \frac{1}{2\pi\sigma_x\sigma_y\sqrt{1-\rho^2}} \times \exp\left[-\frac{1}{2(1-\rho^2)} \left[\left(\frac{x-\mu_x}{\sigma_x}\right)^2 + \left(\frac{y-\mu_y}{\sigma_y}\right)^2 - 2\rho\left(\frac{x-\mu_x}{\sigma_x}\right)\left(\frac{y-\mu_y}{\sigma_y}\right) \right]\right]. \quad (4)$$

The above PDF has a maximum at the mean vector (μ_x, μ_y) . The contours of equal density of bivariate normal distribution are ellipses at (μ_x, μ_y) . The major axes of these ellipses have a positive slope when ρ is positive, and a negative slope when ρ is negative. If $\rho = 0$, these contours are circles.

Notice that x and y can be written in polar coordinates as $x = r \cos \phi$ and $y = r \sin \phi$, where r is the non-negative RV that represents the radial displacement, and ϕ is an angle in the interval $(-\frac{\pi}{2}, \frac{\pi}{2})$. In order to include the effect of correlated sways in this analysis, we define two new RVs such as x' and y' , which are statistically independent and whose statistics, i.e., mean and variance, will be expressed as a function of the correlation coefficient ρ between x and y . In this way, let us also define these new RVs in polar coordinates as $x = r \cos \phi'$ and $y = r \sin \phi'$, where $\phi_0 = \phi - \phi'$. It must be noted that the relation $x^2 + y^2 = x'^2 + y'^2 = r^2$ always holds, as in [15]. Now, we obtain the ϕ_0 value that makes the covariance between x' and y' equal zero since both of them are statistically independent. Note that the relations $x = x'$ and $y = y'$ also hold when $\phi = \phi'$. Hence, we can write the covariance between x' and y' as

$$\text{Cov}[x', y'] = \text{Cov}[r \cos(\phi - \phi_0), r \sin(\phi - \phi_0)]. \quad (5)$$

Taking into account the properties of the covariance under linear transformations, we can rewrite the covariance expressed above as follows:

$$\text{Cov}[x', y'] = 2\rho\sigma_x\sigma_y \cos^2 \phi_0 + (\sigma_y^2 - \sigma_x^2) \sin \phi_0 \cos \phi_0 - \rho\sigma_x\sigma_y. \quad (6)$$

TABLE 1
Expressions for Pointing Error Parameters with Correlated Sways

Parameter	Symbol	Expression
Horizontal mean	μ'_x	$\mu_x \cos \phi_0 + \mu_y \sin \phi_0$
Vertical mean	μ'_y	$\mu_y \cos \phi_0 - \mu_x \sin \phi_0$
Horizontal variance	$\sigma_x'^2$	$\sigma_x^2 \cos^2 \phi_0 + \sigma_y^2 \sin^2 \phi_0 + 2\rho\sigma_x\sigma_y \sin \phi_0 \cos \phi_0$
Vertical variance	$\sigma_y'^2$	$\sigma_y^2 \cos^2 \phi_0 + \sigma_x^2 \sin^2 \phi_0 - 2\rho\sigma_x\sigma_y \sin \phi_0 \cos \phi_0$

Therefore, the ϕ_0 values that make the covariance obtained in (6) equal zero, i.e., $\text{Cov}[x', y'] = 0$, are computed as

$$\phi_0 = \begin{cases} \frac{\pi}{4}, & \sigma_x = \sigma_y \\ \frac{1}{2} \arctan \left(\frac{2\rho\sigma_x\sigma_y}{\sigma_x^2 - \sigma_y^2} \right), & \sigma_x \neq \sigma_y. \end{cases} \quad (7)$$

For even further detail, Appendix A shows how the ϕ_0 value was obtained. At this time, we can derive the corresponding means and variances of x' and y' , which have been derived in appendix B and, further, are shown as a summary in Table 1. Similar to (3), we can express both x' and y' in a matrix form as follows:

$$\begin{pmatrix} x' \\ y' \end{pmatrix} \sim N \left[\begin{pmatrix} \mu'_x \\ \mu'_y \end{pmatrix}, \begin{pmatrix} \sigma_x'^2 & 0 \\ 0 & \sigma_y'^2 \end{pmatrix} \right]. \quad (8)$$

Finally, it must be noted that the radial displacement r at the receiver plane is expressed as $r^2 = x'^2 + y'^2$, where x' and y' represent the equivalent horizontal displacement and the equivalent elevation, respectively. Both x' and y' are modeled as independent Gaussian RVs with unequal means and unequal variances.

2.1 Linear Correlation Analysis

In the light of expressions obtained in Table 1, different conclusions can be drawn from the transformation of Gaussian RVs performed here in order to add the effect of correlated sways to the generalized misalignment fading. First, it must be noted that both boresight errors and pointing error deviations corresponding to the horizontal displacement and the elevation strongly depend on the correlation coefficient. This fact makes a transformation in PDFs that needs to be addressed.

When the radial displacement follows a Rayleigh distribution, i.e., $\mu_x = \mu_y = 0$ and $\sigma_x = \sigma_y$, the effect of correlated sways turns a Rayleigh distribution into a Hoyt distribution. The effect of correlation makes different jitters in each axis. At the same time, when the radial displacement follows a lognormal-Rice distribution, i.e., $\mu_x \neq \mu_y \neq 0$ and $\sigma_x = \sigma_y$, the effect of correlated sways turns a lognormal-Rice distribution into a Beckmann distribution, i.e., the most general case, where each of parameters can take different values. This phenomenon does not occur in the rest of distributions such as Hoyt and Beckmann, i.e., $\sigma_x \neq \sigma_y$, due to the fact that both of them assume different jitters and, hence, the effect of correlation keeps making the same PDF. According to Table 1, the corresponding expressions of jitter variances are plotted in Fig. 1 in order to see how these variances are affected by the effect of correlation when these ones start taking the same value (the figure on the left), or different values (the figure on the right). Note that this figure does not depend on atmospheric turbulence. The most relevant thing here is that when one axis increases,

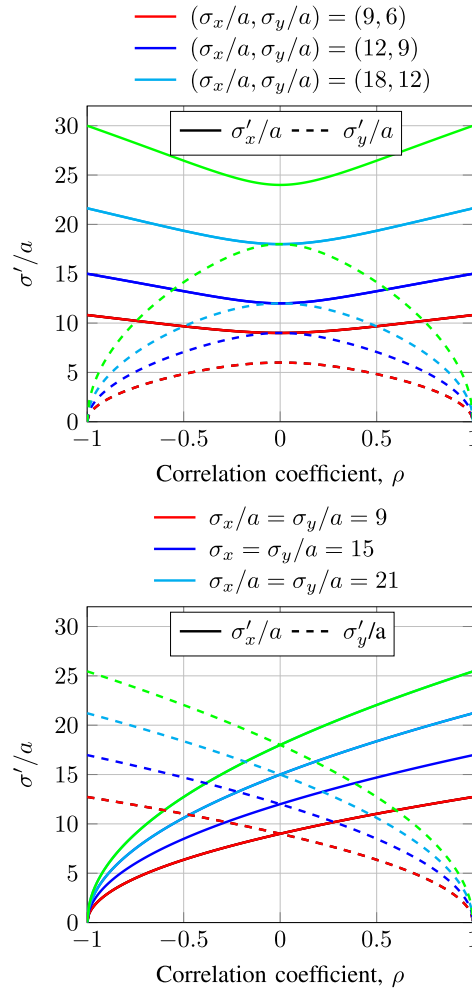


Fig. 1. Effect of correlation on normalized jitters as a function of the correlation coefficient ρ for a FSO link distance of $d_{SD} = 3$ km.

the another one does the opposite, increasing the dispersion between both axes, as well as the symmetry with respect to $\rho = 0$.

3. System and Channel Models

3.1 System Model

Let us consider a single-input/single-output (SISO) FSO link that is based on intensity-modulation and direct-detection (IM/DD) due to their simplicity and low cost, and on-off keying (OOK) modulation. In this way, the received electrical signal for a SISO FSO link is given by

$$y = hRx + z \quad (9)$$

where R is the detector responsivity, assumed hereinafter to be the unity, x is the transmitted optical power, h is the equivalent real-value fading gain of the channel between the source and the receiver, and z is additive white Gaussian noise (AWGN) with zero mean and variance $\sigma_n^2 = N_0/2$. The channel gain is a product of three factors, i.e., $h = L \cdot h_a \cdot h_p$, atmospheric path loss L , atmospheric turbulence h_a , and geometric spread and pointing errors h_p . Note that both atmospheric turbulence and pointing errors are considered to be statistically independent. The path loss L is determined

by the exponential Beers-Lambert law as $L = e^{-\Phi d_{SD}}$, where d_{SD} is the link distance and Φ is the atmospheric attenuation coefficient described in [16]. The received electrical signal-to-noise ratio (SNR) can be defined as $\gamma_T = 4\gamma h^2$, where $\gamma = P_t^2 T_b / N_0$ is the normalized received electrical SNR in absence of turbulence, P_t is the average transmitted optical power, and T_b is the bit period.

3.2 Channel Model

As recently presented in [11], where a new approximation was proposed to efficiently study pointing errors modeled by the Beckmann distribution, we take full advantage of this approximation due to its mathematical simplicity to include the effect of correlated sways. The PDF of h_p is approximated, as in [11], as

$$f_{h_p}(h) \simeq \frac{\varphi_{\text{mod}}^2}{A_{\text{mod}} \varphi_{\text{mod}}^2} h^{\varphi_{\text{mod}}^2 - 1}, \quad 0 \leq h \leq A_{\text{mod}} \quad (10)$$

where $\varphi_{\text{mod}} = \omega_{z_{\text{eq}}} / 2\sigma_{\text{mod}}$. The authors derived an approximation of the PDF of r that is based on a modified Rayleigh distribution of one parameter: σ_{mod}^2 . The corresponding expression of σ_{mod}^2 was obtained in [11, Eq. (9)] as

$$\sigma_{\text{mod}}^2 = \left(\frac{3\mu_x'^2 \sigma_x'^4 + 3\mu_y'^2 \sigma_y'^4 + \sigma_x'^6 + \sigma_y'^6}{2} \right)^{1/3}. \quad (11)$$

Also, the corresponding expression of A_{mod} was obtained in [11, Eq. (15)] as

$$A_{\text{mod}} = A_0 \exp \left(\frac{1}{\varphi_{\text{mod}}^2} - \frac{1}{2\varphi_x'^2} - \frac{1}{2\varphi_y'^2} - \frac{\mu_x'^2}{2\sigma_x'^2 \varphi_x'^2} - \frac{\mu_y'^2}{2\sigma_y'^2 \varphi_y'^2} \right). \quad (12)$$

Note that both σ_{mod}^2 and A_{mod} are computed by using the corresponding statistics of x' and y' , as can be seen in Table 1. A closed-form expression of the combined PDF was derived in [11, (16)] when the radial displacement r is determined by a modified Rayleigh distribution. Therefore, that expression can be used to compute the combined effect of the GG atmospheric turbulence and generalized pointing errors taking correlated sways into account. Therefore, the PDF is approximated as follows:

$$f_h(h) \simeq \frac{\alpha\beta\varphi_{\text{mod}}^2 h^{-1}}{A_{\text{mod}} L \Gamma(\alpha)\Gamma(\beta)} G_{1,3}^{3,0} \left(\frac{\alpha\beta}{A_{\text{mod}} L} h \left| \begin{array}{c} \varphi_{\text{mod}}^2 + 1 \\ \varphi_{\text{mod}}^2, \alpha, \beta \end{array} \right. \right), \quad h \geq 0 \quad (13)$$

where $G_{p,q}^{m,n}[\cdot]$ is the Meijer's G-function [17]. The corresponding cumulative distribution function (CDF) is derived using [18, (07.34.21.0001.01)] as

$$F_h(h) \simeq \frac{\varphi_{\text{mod}}^2}{\Gamma(\alpha)\Gamma(\beta)} G_{2,4}^{3,1} \left(\frac{\alpha\beta}{A_{\text{mod}} L} h \left| \begin{array}{c} 1, \varphi_{\text{mod}}^2 + 1 \\ \varphi_{\text{mod}}^2, \alpha, \beta, 0 \end{array} \right. \right), \quad h \geq 0. \quad (14)$$

Assuming negligible inner scale, α and β can directly be linked to physical parameters through the following expressions [19]:

$$\alpha = \left[\exp \left(\frac{0.49\chi^2}{(1 + 0.18d^2 + 0.56\chi^{12/5})^{7/6}} \right) - 1 \right]^{-1} \quad (15a)$$

$$\beta = \left[\exp \left(\frac{0.51\chi^2(1 + 0.69\chi^{12/5})^{-5/6}}{(1 + 0.9d^2 + 0.62d^2\chi^{12/5})^{5/6}} \right) - 1 \right]^{-1} \quad (15b)$$

where $\chi^2 = 0.4\sigma_R^2 = 0.5\kappa^{7/6} C_n^2 d_{SD}^{11/6}$ is the Rytov variance for a spherical wave, which is a measure of the optical turbulence strength, and $d^2 = \kappa D^2 / 4d_{SD}$. Here, $\kappa = 2\pi/\lambda$ is the optical wave number, λ is the wavelength, $D = 2a$ is the diameter of the receiver collecting lens aperture, d_{SD} is the source-destination link distance, and C_n^2 is the refractive index structure parameter. It must be emphasized

that α and β cannot arbitrarily be chosen in FSO applications due to the fact that both parameters are related to the Rytov variance.

4. Performance Analysis of Terrestrial FSO Links with Correlated Sways

4.1 Outage Performance Analysis

In this section, the effect of correlated sways on outage performance over GG atmospheric channels is carefully analyzed. Outage probability, P_{out} , can be defined as the probability that the instantaneous combined SNR, γ_T , falls below a certain specified threshold, γ_{th} , which is a protection value of the SNR above which the quality of the channel is satisfactory as

$$P_{\text{out}} := P(\gamma_T \leq \gamma_{th}) = \int_0^{\gamma_{th}} f_{\gamma_T}(\gamma) d\gamma. \quad (16)$$

By using (16), the outage probability can be written as

$$\begin{aligned} P_{\text{out}} &= P(\gamma_T \leq \gamma_{th}) = P(4\gamma h^2 \leq \gamma_{th}) = \int_0^{\sqrt{\gamma_{th}/4\gamma}} f_h(h) dh = F_h\left(\sqrt{\frac{\gamma_{th}}{4\gamma}}\right) \\ &= \frac{\varphi_{\text{mod}}^2}{\Gamma(\alpha)\Gamma(\beta)} G_{2,4}^{3,1}\left(\frac{\alpha\beta}{A_{\text{mod}}L} \sqrt{\frac{\gamma_{th}}{4\gamma}} \middle| \begin{matrix} 1, \varphi_{\text{mod}}^2 + 1 \\ \varphi_{\text{mod}}^2, \alpha, \beta, 0 \end{matrix}\right). \end{aligned} \quad (17)$$

In order to reveal more insights into this challenging analysis, the corresponding Maclaurin series expansion of the Meijer's G-function [18, (07.34.06.0006.01)] is used here as follows:

$$P_{\text{out}} \doteq \begin{cases} \frac{\varphi_{\text{mod}}^2(\alpha\beta)^{\min(\alpha,\beta)}\Gamma(|\alpha-\beta|)}{\min(\alpha,\beta)(A_{\text{mod}}L)^{\min(\alpha,\beta)}\Gamma(\alpha)\Gamma(\beta)(\varphi_{\text{mod}}^2 - \min(\alpha,\beta))} \left(\frac{\gamma_{th}}{4\gamma}\right)^{\min(\alpha,\beta)/2}, & \varphi_{\text{mod}}^2 > \min(\alpha,\beta) \\ \frac{\varphi_{\text{mod}}^2(\alpha\beta)^{\varphi_{\text{mod}}^2}\Gamma(\alpha - \varphi_{\text{mod}}^2)\Gamma(\beta - \varphi_{\text{mod}}^2)}{\varphi_{\text{mod}}^2(A_{\text{mod}}L)^{\varphi_{\text{mod}}^2}\Gamma(\alpha)\Gamma(\beta)} \left(\frac{\gamma_{th}}{4\gamma}\right)^{\varphi_{\text{mod}}^2/2}, & \varphi_{\text{mod}}^2 < \min(\alpha,\beta). \end{cases} \quad (18)$$

It is straightforward to show that the outage probability behaves asymptotically as $P_{\text{out}} \doteq (O_c\gamma)^{-O_d}$, where O_d and O_c denote outage diversity and coding gain, respectively [20]. At high SNR, the outage diversity determines the slope of the outage probability versus average SNR curve in a log-log scale and the coding gain (in decibels) determines the shift of the curve in SNR. Hence, it can be deduced from (18) that the outage diversity for a FSO link under the presence on generalized pointing errors with correlated sways is expressed as follows:

$$O_d = \min(\alpha, \beta, \varphi_{\text{mod}}^2) / 2 \quad (19)$$

where the effect of correlated sways appears to be implicitly in φ_{mod}^2 .

4.2 Numerical Results

Now, the effect of correlated sways is evaluated over different atmospheric turbulence conditions and different misalignment error values.

Note that the system configuration adopted in this study is used in most practical terrestrial FSO communication systems [5], [6], as shown in Table 2. Different weather conditions are adopted in this paper: haze visibility of 4 km with $C_n^2 = 2 \times 10^{-14} \text{ m}^{-2/3}$ and clear visibility of 16 km with $C_n^2 = 8 \times 10^{-14} \text{ m}^{-2/3}$, corresponding to moderate and strong turbulence conditions, respectively. A wavelength value of $\lambda = 1550 \text{ nm}$ is chosen due to its low attenuation as well as the proliferation of high-quality transmitter and detector components. A source-destination link distance of $d_{SD} = 3 \text{ km}$ is assumed together with a $D = 10 \text{ cm}$ receiver aperture in order to study a practical FSO communications system, wherein the typical link distance values are between 1–5 km, as well as typical values for the receiver diameter are on the order of 5–20 cm. Rytov variance values of $\chi^2 = \{1.2, 4.8\}$ for spherical wave are derived for $d_{SD} = 3 \text{ km}$ corresponding to moderate and strong

TABLE 2
FSO Communication System Settings

Parameter	Symbol	Value
FSO link distance	d_{SD}	3 km
Wavelength	λ	1550 nm
Receiver aperture diameter	$D = 2a$	10 cm
Transmit divergence	θ_z	1 mrad
Normalized beam width	ω_z/a	$\simeq 60$
Maximum jitter angle	$(\theta_{sx}, \theta_{sy})$	0.4 mrad
Maximum normalized jitter	$(\sigma_x/a, \sigma_y/a)$	$\simeq 24$
Maximum boresight angle	$(\theta_{bx}, \theta_{by})$	0.3 mrad
Maximum normalized boresight error	$(\mu_x/a, \mu_y/a)$	$\simeq 18$

turbulence, respectively. Regarding pointing error values, a narrower beam width should be used to avoid a high geometric loss when link distances greater than one kilometer are assumed. In this case, the use of automatic pointing and tracking systems is required in order to reduce pointing error effects, typically between 0.05-1 mrad of divergence at $1/e^2$ that is equivalent to a beam spread of 15–300 cm at 3 km [5], [6]. At the same time, different jitter variances are used to study the outage performance, which can take values up to 0.4 mrad, as well as different nonzero boresight errors, which can take values up to 0.1 mrad or even much smaller [4]. Parameters α and β are calculated from (15).

1) *Outage Diversity Analysis*: For a better understanding of the impact of correlated sways on outage performance of FSO links, the outage diversity obtained in (19) is depicted in Fig. 2 as a function of the linear correlation coefficient ρ for different normalized jitter values as well as different normalized boresight error values, which are both obtained according to Table 2. A normalized beam width value of $\omega_z/a = 60$ is derived according to the FSO link distance considered in this analysis. In the light of (19), we can know what issue, i.e., atmospheric turbulence or pointing errors, is the dominant effect. From Fig. 2, it can be observed that the outage diversity is strongly dependent on the correlation coefficient. As expected, when atmospheric turbulence is the dominant effect, i.e., when normalized jitter values of $\sigma_x/a = \sigma_y/a = 6$ are considered, the outage diversity keeps at a constant level due to the fact that atmospheric turbulence does not depend on correlation coefficient. On the contrary, when pointing error is the dominant effect, i.e., when normalized jitter values of $\sigma_x/a = \sigma_y/a = \{15, 18, 21\}$ are considered, the outage diversity strongly depends on the correlation coefficient. In other words, the relation $\varphi_{\text{mod}}^2 > \min(\alpha, \beta)$ does not hold when larger amounts of misalignment are assumed, such as $\sigma_x/a = \sigma_y/a = \{15, 18, 21\}$.

Note that the pointing error values used in Fig. 2, i.e., pointing error values that are used as described in the legend to Fig. 2, are the input parameters in the FSO system together with other ones such as FSO link distance, wavelength, among others. As previously commented in Section 2, the effect of correlated sways turns a initial PDF into another one. This fact, for instance, can be observed in Fig. 2 where normalized jitter values for the horizontal displacement and the elevation start taking the same value, but the effect of correlation makes different jitters in each axis as corroborated in Fig. 1. This phenomenon is more pronounced under high correlation conditions. More specifically, we can see in Fig. 2(a) as the effect of correlated sways turns a Rayleigh distribution into a Hoyt distribution and, hence, the outage diversity decreases as the correlation coefficient increases since the dispersion between both sigma values increase. At the same time, we can also see a similar behavior in Figs. 2(b) and (c), where a lognormal-Rice distribution turns into a

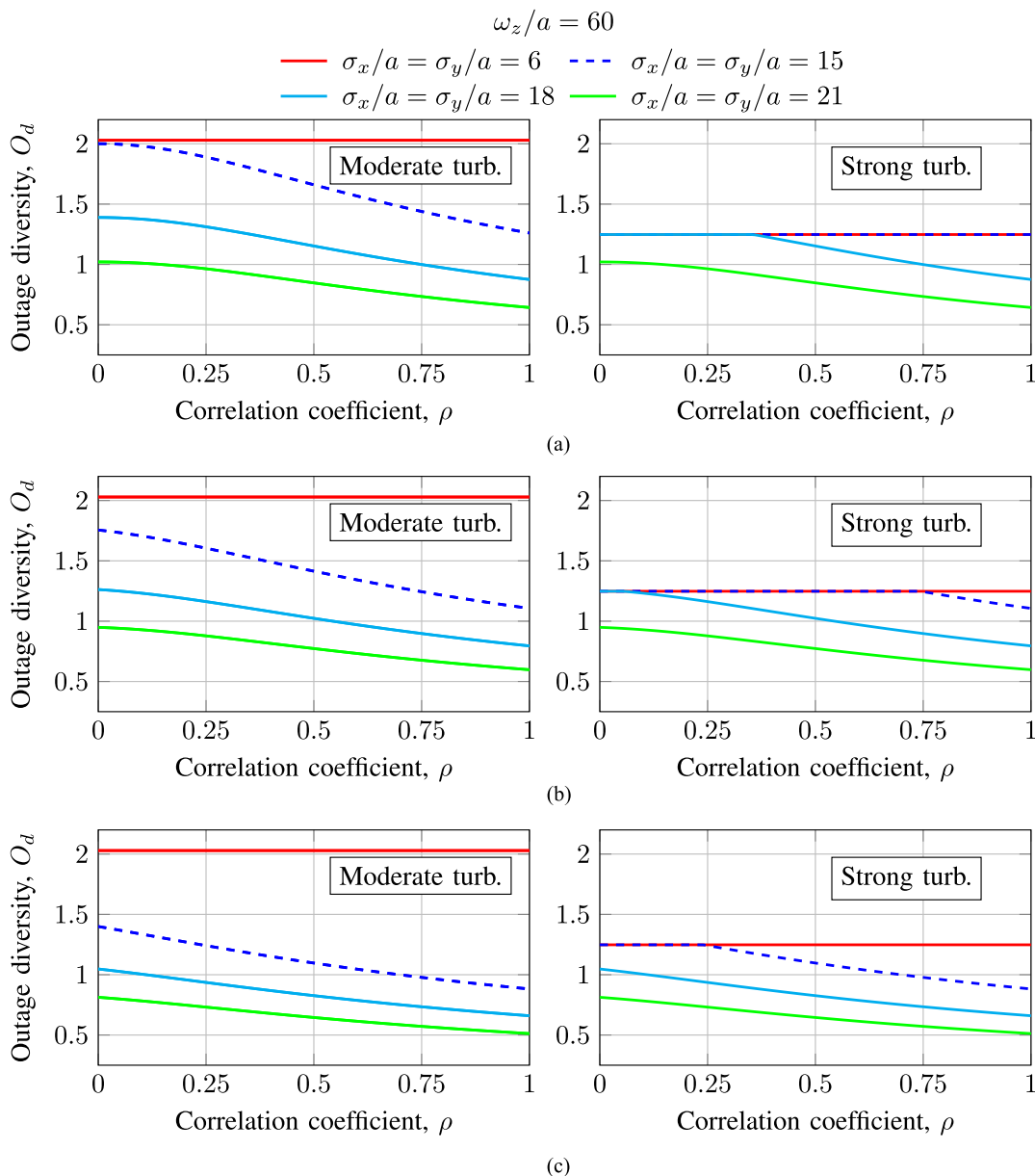


Fig. 2. Outage diversity O_d as a function of the correlation coefficient ρ for a FSO link distance of $d_{SD} = 3$ km and different normalized boresight error values when a normalized beam width value of $\omega_z/a = 60$ is assumed. (a) Zero boresight. (b) $\mu_x/a = \mu_y/a = 6$. (c) $\mu_x/a = \mu_y/a = 12$.

Beckmann distribution taking into account the effect of boresight errors. In this case, the outage diversity degrades more rapidly with larger amounts of misalignment.

More importantly, generalized pointing errors with correlated sways can make a change in the dominant effect, mainly under strong turbulence conditions. For instance, it can be observed in Fig. 2(b) under strong turbulence that the outage diversity is flat for normalized jitter values of $\sigma_x/a = \sigma_y/a = 6$, which means that this one is determined by atmospheric turbulence. But, the outage diversity is also flat up to a correlation coefficient value of $\rho \approx 0.75$ for normalized jitter values of $\sigma_x/a = \sigma_y/a = 15$, which means that the outage diversity is determined by atmospheric turbulence up to that value. The outage diversity starts being determined by pointing errors for correlation coefficient values greater than ≈ 0.75 . This is a clear example of how the effect of

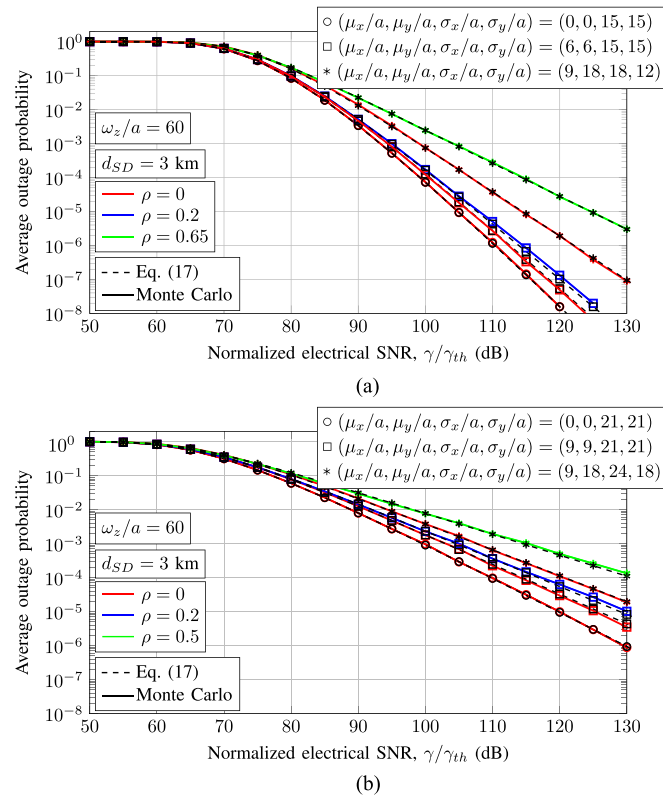


Fig. 3. Outage performance over GG atmospheric turbulence and generalized misalignment fading channels with correlated sways, when different weather conditions (a) $C_n^2 = 2 \times 10^{-14} \text{ m}^{-2/3}$ and (b) $C_n^2 = 8 \times 10^{-14} \text{ m}^{-2/3}$ are assumed for a FSO link distance of $d_{SD} = 3 \text{ km}$ and different correlation values. (a) Moderate turbulence. (b) Strong turbulence.

correlated sways can make a change in the dominant effect. The same conclusions can also be drawn from Figs. 2(a) and (c). This phenomenon happens much more frequently under strong turbulence than moderate turbulence due to the fact that both α and β take smaller values.

2) *Outage Performance Analysis:* The corresponding results of this outage performance analysis are illustrated in Fig. 3(a) for moderate turbulence and Fig. 3(b) for strong turbulence as a function of the inverse normalized threshold SNR, γ/γ_{th} .

In order to confirm the accuracy and usefulness of the proposed approximation given in (17), Monte Carlo simulation results, where the FSO link is modeled by using the statistical model given in (9), are further included by using solid line generating the corresponding variates from the exact combined PDF. Due to the long simulation time involved, simulation results only up to 10^{-8} are included in Fig. 3. It is noteworthy to mention that the results obtained by using the proposed approximate expression provide quite a good match between the analytical and the respective Monte Carlo simulation results.

With the goal of analyzing the effect of correlated sways on outage performance, different correlation coefficient values are considered in Fig. 3 such as $\rho = \{0, 0.2, 0.65\}$ and $\rho = \{0, 0.2, 0.5\}$ for moderate and strong turbulence conditions, respectively. Additionally, the uncorrelated case, i.e., uncorrelated sways, is also included in Fig. 3 as a reference. As in Fig. 2, the pointing error values used in Fig. 3, i.e., pointing error values that are used as described in the legend to Fig. 3, are the input parameters in the FSO system. In this way, simulation and analytical results, which are illustrated by using red color, represent the uncorrelated cases when the radial displacement follows a Rayleigh distribution, a lognormal-Rice distribution and a Beckmann distribution (by using different marks). At the same time, two different correlated cases are depicted. On the one hand,

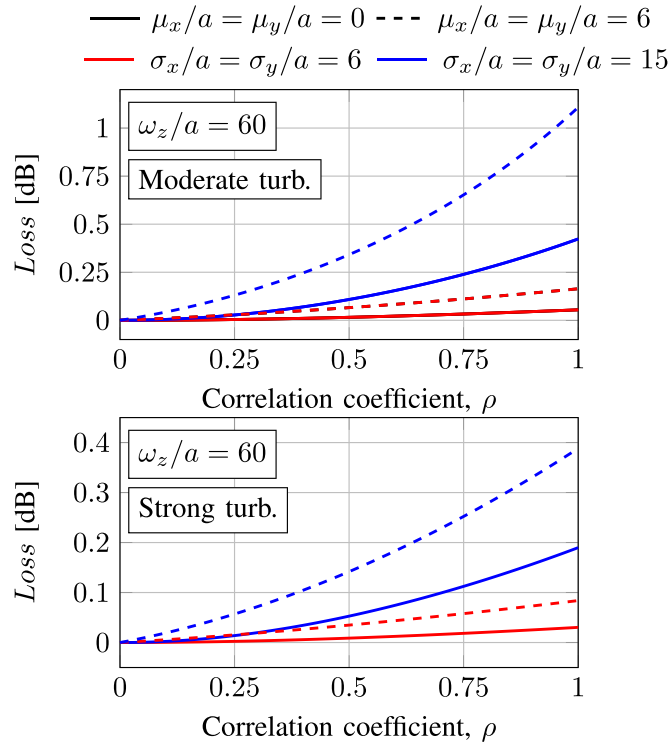


Fig. 4. Loss, i.e., L_{oss} [dB], as a function of the correlation coefficient for a link distance of $d_{SD} = 3$ km and different jitter variances and normalized boresight error values.

when the radial displacement follows a lognormal-Rice distribution, the effect of correlated sways makes this PDF turns into a Beckmann distribution, which is illustrated by using blue color. On the other hand, when the radial displacement follows a Beckmann distribution, the effect of correlated sways keeps making the same distribution but the statistical parameters take different values, which is illustrated by using green color. As expected, the obtained outage performance is strongly dependent on the effect of correlated sways. When a nonzero correlation coefficient or larger amounts of misalignment are assumed, the outage performance is remarkably decreased. This shows that the effect of correlated sways cannot be ignored since this one presents a strong impact not only on the outage diversity when pointing error is the dominant effect, as shown in the previous figure, but on the coding gain when atmospheric turbulence is the dominant effect as well.

4.3 Impact of Correlation on Coding Gain

Taking into account the coding gain O_c in (18), the impact of correlated sways translates into a loss, i.e., L_{oss} [dB], relative to GG atmospheric turbulence without considering correlated sways given by

$$L_{oss} [dB] \triangleq O_c^{\rho \neq 0} [dB] - O_c^{\rho = 0} [dB]. \quad (20)$$

The above expression computes the additional power needed to obtain a given outage performance when there is correlation versus no correlation. The above expression is plotted in Fig. 4 as a function of the correlation coefficient for a FSO link distance of $d_{SD} = 3$ km and a normalized beam width value of $\omega_z/a = 60$ under the condition that atmospheric turbulence is the dominant effect, i.e., the outage diversity is only determined by turbulence.

It can be observed that the losses slightly increase as the correlation coefficient does regardless of the severity of atmospheric turbulence. Nevertheless, the impact of correlation on coding gain

is more remarkable for moderate turbulence than strong turbulence. As expected, a greater loss is obtained when nonzero boresight errors are considered.

5. Conclusion

An in-depth analysis of the effect of correlated sways on generalized misalignment fading for terrestrial FSO links is carried out in order to readily study how such effect impacts on the outage performance over GG atmospheric turbulence channels. There are no papers that address this research problem in the literature. Motivated by the above, the authors have made an effort to fill up this gap.

From this study, we can conclude that the impact of correlated sways on the outage performance cannot be ignored in terrestrial FSO applications since the horizontal displacement and the elevation are not necessarily uncorrelated RVs. Interestingly, the effect of correlation turns a PDF into another one. In other words, the effect of correlation makes that the corresponding statistical distribution of the radial displacement at the receiver turns to another one when the correlation coefficient takes values different from zero. This phenomenon is really interesting since two pointing error models might be assumed taking into account the effect of correlated sways such as Rayleigh (zero boresight case) distribution and lognormal-Rice (nonzero boresight case) distribution. The correlation makes that both statistical distributions turn to other ones more real when the correlation coefficient does not equal zero, obtaining a Hoyt distribution and a Beckmann distribution, respectively. Additionally, from an asymptotic point of view, the effect of correlation presents a strong impact not only on the outage diversity when pointing error is the dominant effect, but on the coding gain when atmospheric turbulence is the dominant effect.

Last, but not least, it is also concluded that the approximate closed-form expression obtained here for the outage probability is valid for research on performance of any kind of FSO system under the presence of generalized pointing errors with correlated sways. Moreover, this work can be extended to other atmospheric statistical models such as LN for weak turbulence and EW considering the effect of aperture averaging. We believe that these results open a new way of thinking when designing FSO systems, adding a higher degree of sophistication and realism to the FSO system model. Further, an experimental verification of this pointing error model may be a promising line for future research.

Appendix A

In this Appendix, we find the corresponding ϕ_0 value that ensures that the following equation is right:

$$2\rho\sigma_x\sigma_y \cos^2 \phi_0 + (\sigma_y^2 - \sigma_x^2) \sin \phi_0 \cos \phi_0 - \rho\sigma_x\sigma_y = 0. \quad (21)$$

We can write the above expression as follows:

$$\frac{2 \sin \phi_0 \cos \phi_0}{2 \cos^2 \phi_0 - 1} = \frac{2\rho\sigma_x\sigma_y}{\sigma_x^2 - \sigma_y^2}. \quad (22)$$

Notice that [17, (1.313.9)]

$$\tan 2a = \frac{2 \tan a}{1 - \tan^2 a} = \frac{2 \sin a \cos^2 a}{2 \cos^2 a - 1}. \quad (23)$$

We can rewrite the expression in (22) taking into account the above expression as follows:

$$\tan 2\phi_0 = \frac{2\rho\sigma_x\sigma_y}{\sigma_x^2 - \sigma_y^2}. \quad (24)$$

The ϕ_0 values that make the covariance obtained in (6) equals zero, i.e., $Cov[x', y'] = 0$, are computed as

$$\phi_0 = \begin{cases} \frac{\pi}{4}, & \sigma_x = \sigma_y \\ \frac{1}{2} \arctan\left(\frac{2\rho\sigma_x\sigma_y}{\sigma_x^2 - \sigma_y^2}\right), & \sigma_x \neq \sigma_y. \end{cases} \quad (25)$$

Appendix B

In this Appendix, we derive the corresponding means and variances of x' and y' , which are modeled as independent Gaussian RVs with unequal means and unequal variances. In this way, the corresponding mean of x' can easily be obtained as follows:

$$\begin{aligned} \mu'_x &= \mathbb{E}[x'] = \mathbb{E}[r \cos(\phi - \phi_0)] = \mathbb{E}[r \cos \phi \cos \phi_0 + r \sin \phi \sin \phi_0] \\ &= \cos \phi_0 \mathbb{E}[r \cos \phi] + \sin \phi_0 \mathbb{E}[r \sin \phi] = \mu_x \cos \phi_0 + \mu_y \sin \phi_0. \end{aligned} \quad (26)$$

Similar to the above expression, the corresponding mean of y' is also obtained as follows:

$$\begin{aligned} \mu'_y &= \mathbb{E}[y'] = \mathbb{E}[r \sin(\phi - \phi_0)] = \mathbb{E}[r \sin \phi \cos \phi_0 - r \cos \phi \sin \phi_0] \\ &= \cos \phi_0 \mathbb{E}[r \sin \phi] - \sin \phi_0 \mathbb{E}[r \cos \phi] = \mu_y \cos \phi_0 - \mu_x \sin \phi_0. \end{aligned} \quad (27)$$

Finally, the corresponding variance of x' can be obtained by performing some easy algebraic manipulations as follows:

$$\begin{aligned} \sigma_x'^2 &= \text{Var}[x'] = \text{Var}[r \cos(\phi - \phi_0)] = \text{Var}[r \cos \phi \cos \phi_0 + r \sin \phi \sin \phi_0] \\ &= \cos^2 \phi_0 \text{Var}[r \cos \phi] + \sin^2 \phi_0 \text{Var}[r \sin \phi] \\ &\quad + 2 \cos \phi_0 \sin \phi_0 \text{Cov}[r \cos \phi, r \sin \phi] \\ &= \sigma_x^2 \cos^2 \phi_0 + \sigma_y^2 \sin^2 \phi_0 + 2\rho\sigma_x\sigma_y \sin \phi_0 \cos \phi_0. \end{aligned} \quad (28)$$

Similar to the above expression, the corresponding variance of y' is also obtained as follows:

$$\begin{aligned} \sigma_y'^2 &= \text{Var}[y'] = \text{Var}[r \sin(\phi - \phi_0)] = \text{Var}[r \sin \phi \cos \phi_0 - r \cos \phi \sin \phi_0] \\ &= \cos^2 \phi_0 \text{Var}[r \sin \phi] + \sin^2 \phi_0 \text{Var}[r \cos \phi] \\ &\quad - 2 \cos \phi_0 \sin \phi_0 \text{Cov}[r \sin \phi, r \cos \phi] \\ &= \sigma_y^2 \cos^2 \phi_0 + \sigma_x^2 \sin^2 \phi_0 - 2\rho\sigma_x\sigma_y \sin \phi_0 \cos \phi_0. \end{aligned} \quad (29)$$

References

- [1] M. A. Khalighi and M. Uysal, "Survey on free space optical communication: A communication theory perspective," *IEEE Commun. Surveys Tuts.*, vol. 16, no. 4, pp. 2231–2258, Fourth Quar. 2014.
- [2] S. Arnon, "Effects of atmospheric turbulence and building sway on optical wireless-communication systems," *Opt. Lett.*, vol. 28, no. 2, pp. 129–131, 2003.
- [3] A. K. Majumdar and J. C. Ricklin, *Free-Space Laser Communications: Principles and Advances*, vol. 2. New York, NY, USA: Springer, 2010.
- [4] D. K. Borah and D. G. Voelz, "Pointing error effects on free-space optical communication links in the presence of atmospheric turbulence," *J. Lightw. Technol.*, vol. 27, no. 18, pp. 3965–3973, Sep. 15, 2009.
- [5] I. I. Kim *et al.*, "Wireless optical transmission of fast Ethernet, FDDI, ATM, and ESCON protocol data using the teralink laser communication system," *Opt. Eng.*, vol. 37, no. 12, pp. 3143–3155, 1998.
- [6] S. Bloom, E. Korevaar, J. Schuster, and H. Willebrand, "Understanding the performance of free-space optics [Invited]," *J. Opt. Netw.*, vol. 2, no. 6, pp. 178–200, 2003.
- [7] A. A. Farid and S. Hranilovic, "Outage capacity optimization for free-space optical links with pointing errors," *J. Lightw. Technol.*, vol. 25, no. 7, pp. 1702–1710, Jul. 2007.
- [8] W. Gappmair, S. Hranilovic, and E. Leitgeb, "OOK performance for terrestrial FSO links in turbulent atmosphere with pointing errors modeled by Hoyt distributions," *IEEE Commun. Lett.*, vol. 15, no. 8, pp. 875–877, Aug. 2011.

- [9] F. Yang, J. Cheng, and T. Tsiftsis, "Free-space optical communication with nonzero boresight pointing errors," *IEEE Trans. Commun.*, vol. 62, no. 2, pp. 713–725, Feb. 2014.
- [10] H. AlQuwaiee, H. C. Yang, and M. Alouini, "On the asymptotic capacity of dual-aperture FSO systems with a generalized pointing error model," *IEEE Trans. Wireless Commun.*, vol. 15, no. 9, pp. 6502–6512, Sep. 2016.
- [11] R. Boluda-Ruiz, A. García-Zambrana, C. Castillo-Vázquez, and B. Castillo-Vázquez, "Novel approximation of misalignment fading modeled by Beckmann distribution on free-space optical links," *Opt. Exp.*, vol. 24, no. 20, pp. 22635–22649, Oct. 2016.
- [12] R. Boluda-Ruiz, A. García-Zambrana, C. del Castillo-Vázquez, B. del Castillo-Vázquez, and S. Hranilovic, "Outage performance of exponentiated Weibull FSO links under generalized pointing errors," *J. Lightw. Technol.*, 2017, to be published.
- [13] X. Liu, "Optimisation of satellite optical transmission with correlated sways," *IET Commun.*, vol. 5, no. 8, pp. 1107–1112, 2011.
- [14] X. Liu, "Performance analysis of a multiple-input-single-output optical satellite communication system with correlated pointing errors," *IET Commun.*, vol. 6, no. 15, pp. 2503–2511, 2012.
- [15] P. Beckmann, "Statistical distribution of the amplitude and phase of a multiply scattered field," *J. Res. NBS D*, vol. 66, pp. 231–240, 1962.
- [16] I. I. Kim, B. McArthur, and E. J. Korevaar, "Comparison of laser beam propagation at 785 nm and 1550 nm in fog and haze for optical wireless communications," in *Proc. Inf. Technol.*, 2001, pp. 26–37.
- [17] I. S. Gradshteyn and I. M. Ryzhik, *Table of Integrals, Series and Products*, 7th ed. San Francisco, CA, USA: Academic, 2007.
- [18] Wolfram Research, Inc. The Wolfram functions site. [Online]. Available: <http://functions.wolfram.com>.
- [19] M. A. Al-Habash, L. C. Andrews, and R. L. Phillips, "Mathematical model for the irradiance probability density function of a laser beam propagating through turbulent media," *Opt. Eng.*, vol. 40, no. 8, pp. 1554–1562, 2001.
- [20] Z. Wang and G. B. Giannakis, "A simple and general parameterization quantifying performance in fading channels," *IEEE Trans. Commun.*, vol. 51, no. 8, pp. 1389–1398, Aug. 2003.